Mikrochim. Acta 127, 131–147 (1997)

Mikrochimica Acta

Fundamental Review

Electrochemistry in Solids Prepared by Sol-Gel Processes

Kathryn S. Alber and **James A. Cox***

Department of Chemistry, Miami University, Oxford, Ohio 45056, U.S.A.

Abstract. Sol-gel chemistry provides a route to preparing inorganic polymers with ionically conducting properties by room temperature synthetic routes. The products, which are rigid solids, are well-suited as media for conventional electrochemical techniques such as cyclic voltammetry. This property, when combined with their ability to host a wide variety of species, has allowed development of a variety of devices of interest in electrochemistry and analytical chemistry. Examples include cathodes for fuels cells, electrochromic devices, biosensors, and amperometric sensors for analytes in the gas phase. In this review, the emphasis will be on reported applications to analytical chemistry; however, studies on the general properties of these materials and on their use in electrochemical science also will be summarized because they may provide the basis for further development of sensors.

Key words: sol-gel chemistry, xerogels, electrochemistry, sensors, biosensors, electrocatalysis, analytical applications

Contents

Introduction 131
Sol-Gel Chemistry 132
  Overview of the Methods of Synthesis 132
  Characterization of the Products 133
Overview of Analytical Applications Using Solids Prepared by Sol-Gel Processes 137
  Spectrophotometric Methods 137
  Bioanalytical Methods Employing Optical Readout 139
  Chromatographic Supports 140
Applications of Sol-Gel Processes to Electrochemistry . . . 140
  Electrochromic Devices 141
  Electrodes for Batteries, Fuel Cells, and General Electrochemistry 141
  Electroanalytical Methods Employing Sol-Gel Chemistry 142
Acknowledgement 145
References 145

Introduction

The preparation of inorganic materials by sol-gel chemistry involves three basic steps. First, a sol, or a dispersion of colloidal particles in a liquid, is prepared. Next, gelation of the sol results in an interconnected, rigid network consisting of submicron pores and polymeric chains. Finally, the solvent is removed to form a condensed solid. The final product can be prepared by a variety of routes and its characteristics can be controlled by selecting the proper experimental conditions along a given route. For instance, the surface area and pore size can be controlled by manipulating the drying procedure of the gel.

Synthesizing inorganic materials by the sol-gel process began as early as the 1840s when Ebelman discovered that a glass-like substance, SiO_2, was formed when tetraethylorthosilicate (TEOS) was hydrolyzed under acidic conditions [1]. In 1864, studies on the structure of inorganic gels supported the theory that a gel consisted of a solid network with continuous porosity [2]. This theory was widely accepted by the 1930s, primarily due to work done by Hurd [3]; he demonstrated that silica gels consisted of a polymeric skeleton of silicic acid that surrounded a liquid phase. The preparation of homogeneous powders, including Al, Si, Ti, and Zr oxides, by sol-gel chemistry was prevalent in the ceramic industry by the 1950s and 1960s, which is exemplified by studies by Roy [4, 5].

---

* To whom correspondence should be addressed

At the same time, the commercial development of colloidal silica powders, DuPont's Ludox spheres, resulted from Iler's research on silica systems [6]. Later, Stober et al. advanced the procedure by demonstrating that the attributes of the powders could be controlled by catalyzing the hydrolysis reaction of TEOS with ammonia [7], which led to a spherical silica powder.

Sol-gel chemistry was advanced when the preparation of multicomponent ceramic materials, based on controlled hydrolysis and condensation of alkoxides, was independently reported by Levene and Thomas [8] and by Dislich [9]. Perhaps the most significant research as a basis of the continuing interest in sol-gel processing, however, was the demonstration in the mid-1970s that monoliths could be produced by cautiously drying the gel [10–12]. Today, the sol-gel process is used to prepare ceramic fibers, coatings, thin films, and numerous other shapes.

Sol-gel processes provide many advantages over conventional ceramic preparation methods. The synthesis is done at low temperatures, which not only simplifies the procedure but allows thermally labile compounds to be entrapped in the sol-gel matrix. Furthermore, the final products are pure and homogeneous, and they can be shaped into a wide variety of forms.

The merits of sol-gel processes are now widely recognized. Inorganic materials prepared by a sol-gel process have been implemented into a variety of technologies, including nonlinear optical devices, luminescent solar concentrators, and chemical sensors. For example, sensor development has relied on immobilizing a sensing molecule, such as an enzyme or a complexing agent, within a sol-gel matrix to provide an inert support for detection purposes.

This review will describe the chemistry involved in sol-gel processes, the experimental conditions that can influence the chemistry, and the properties that evolve during synthesis. Finally, applications to analytical chemistry will be summarized briefly, and a detailed review of application to electrochemistry will be provided.

Sol-Gel Chemistry

Overview of the Methods of Synthesis

Sol-gel processes can be divided into two synthetic routes: aqueous-based methods, that originate with a solution of a metal salt, and alcohol-based methods, which employ an organometallic precursor that is dissolved in the appropriate alcohol. In the first procedure, the initial step is the formation of the sol which occurs when the metal salt is hydrolyzed. In the step that follows, gelation, the formation of the gel occurs by either removing the solvent or increasing the pH. Here, the gel evolves when discrete colloidal particles associate to form a network. However, in the latter procedure, there is no distinct sol-formation step; instead, hydrolysis and condensation reactions progress simultaneously until ultimately a gel is formed. Here, the gel evolves as an interconnected three-dimensional network.

The chronological steps involved in sol-gel processes include hydrolysis, condensation, gelation, aging, drying, and densification or sintering. The primary difference between the two sol-gel methods, which is related to the starting materials, is how the gel is formed. Once gelation takes place, the remaining steps for both procedures are the same. The hydrolysis and condensation of the two types of sol-gel processes are discussed separately below, but the remaining steps that follow are applicable to both methods.

Step 1: Hydrolysis and condensation

Inorganic precursors. Metal cations, M^{n+}, are solvated by water molecules when they are dissolved in pure water and complete hydrolysis occurs when the water reaches a high enough acidity (due to the charge transfer from the water to the cation):

$$M^{n+} + nH_2O \rightarrow M(OH)_n + nH^+$$

Typically, a base is added to force the reaction to the right. Condensation will take place by either nucleophilic substitution,

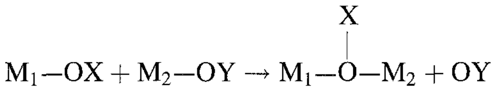

$$M_1{-}OX + M_2{-}OY \rightarrow M_1{-}\overset{X}{\overset{|}{O}}{-}M_2 + OY$$

if the preferred coordination of the metal is satisfied, or by nucleophilic addition,

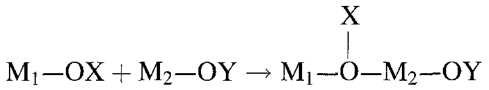

$$M_1{-}OX + M_2{-}OY \rightarrow M_1{-}\overset{X}{\overset{|}{O}}{-}M_2{-}OY$$

if the preferred coordination of the metal is not satisfied to form the sol.

Metal alkoxide precursors. In the alcohol-based process, the sol is formed by hydrolysis of a metal alkoxide precursor,

$$M(OR)_4 + nH_2O \rightarrow M(OR)_{(4-n)}(OH)_n + nHOR$$

and subsequent condensation forms the gel,

$$2M(OR)_{(4-n)}(OH)_n \rightarrow (M(OR)_{(4-n)}(OH)_{(n-1)})_2O + H_2O$$

The hydrolysis is usually catalyzed by an acid or base in an excess of water.

Step 2. Gelation

Inorganic precursors. The sol will spontaneously coagulate to form a gel when the pH is increased (alkaline gelation) or the water is removed (dehydration gelation).

Metal alkoxide precursors. Simultaneous hydrolysis and condensation of the metal alkoxide as described above, gives the overall reaction,

$$M(OR)_4 + 2H_2O \rightarrow MO_2 + 4HOR$$

creating the M–O–M gel network. Regardless of the approach taken to form the gel, it is during gelation that the viscosity increases drastically and a solid is produced.

Aging

Aging occurs if the gel is allowed to set for a period of time in the reaction mixture liquid, resulting in a simultaneous shrinkage of the network. Aging takes place in the following four steps: polymerization, synerisis, coarsening, and phase transformations. Polymerization is characterized by the continuation of condensation reactions and during which the number of linkages increase. Synerisis is the spontaneous shrinkage of the gel and a subsequent expulsion of the liquid from the pores. The dissolution of smaller particles of the gel followed by their reprecipitation onto larger particles occurs during coarsening. In phase transformations, for example, the solid phase can separate from the liquid on a local scale or the liquid can separate into two or more phases. The end result of the aging process is an increase in strength of the gel. It follows that the longer the gel is aged, the stronger the network becomes.

Drying

There are a number of steps involved in removing the liquid from the interconnected pore network during the drying stage. Initially, the solid shrinks by a volume equal to that of the liquid that evaporates; the liquid-vapor interface is only at the exterior surface of the solid. Next, when the solid becomes too stiff to shrink further, the liquid recedes into the interior of the solid where it is isolated into pockets. Further drying can occur only by evaporation of the internal liquid and diffusion of the vapor to the exterior of the solid. A xerogel results when evaporation of the internal liquid occurs under ambient conditions. An aerogel results when removal of the internal liquid is done by supercritical extraction. Excessive capillary stress can cause fracturing during drying and must be avoided.

The sol-gel process can be stopped at the xerogel or the aerogel stage and the "dried gel" can be used for analytical studies. The large surface areas of dried gels combined with their small pore sizes make them unique solids. Xerogels and aerogels are transparent or translucent with typical surface areas of 500–900 m^2/g and $\geq 1000\, m^2/g$, respectively, and nanometer – to Angstrom – scale pore sizes.

Sintering

Sintering is a densification process that is driven by surface energy to eliminate the pores within the gel. In gels, the solid-vapor interfacial area is large, therefore, sintering can be done at relatively low temperatures (e.g., below 1000 °C). The densification tem-perature depends upon the radii of the pores, the degree of connectivity of the pores, and the surface area of the gel. The mechanisms identified for the shrinkage and densification of gels include capillary contraction, condensation, structural relaxation, and viscous sintering. Upon completion of sintering, the gel has been melted and it is now equivalent to a ceramic prepared by conventional means. For use in analytical chemistry, sintering is not commonly done.

Characterization of the Products

It is during the sol-to-gel transition, namely, processing steps 1 and 2 above, that the basic structure of the final product is established. Factors influencing the rates of hydrolysis and condensation reactions are significant because the formation of the sol during these initial steps has implications on the overall gel structure. The most important parameters that affect their kinetics are the temperature, the type (acid or base) and concentration of the catalyst, the type of solvent, the type of alkoxide precursor and the initial mole ratio of alkoxide precursor-to-water (for the alcohol-based method). As temperature of the reaction increases, the rate will also increase. That the catalyst concentration also has a direct linear relationship with the hydrolysis reaction rate was shown by Aelion et al. [13]. In addition, they demonstrated that if the catalyst and matrix were chemically complementary, the rate of hydrolysis was increased. For example, in acidic media the addition of H^+ increased the rate of hydrolysis, whereas in basic media, the addition of OH^- increased the rate of hydrolysis. The nature of the alkoxy group on the metal precursor influences the hydrolysis and condensation reaction rates by decreasing the rate constant when increasing the alkyl group size [14–16]. The ratio of the moles of alkoxide precursor to the moles of water influences the rate of hydrolysis, but a general correlation cannot be made because it varies with each system. Overall, the shape and size of the polymeric backbone of the gel is determined by the ratio of the hydrolysis rate to the condensation rate. Linear polymers form when hydrolysis is fast and condensation is slow, whereas, bulky, large, and highly crosslinked polymers result from slow hydrolysis and fast condensation rates.

The remaining stages of the sol-gel process are influenced by the initial structure of the wet gel in the reaction mixture at the onset of gelation. As described above, gelation occurs by either the aggregation of particles (aqueous-based method) or condensation of polymers to form large clusters (alcohol-based method). The gel point occurs when the clusters link together to form a single unit. At the gel point, the modulus and viscosity of the mixture are the properties that undergo the most drastic change due to the rapid increase in viscosity that causes the gel structure to "set".

A variety of techniques have been used to study the sol-to-gel-to-final product transition. Small-angle scattering methods, including X-ray [17, 18], neutron [19, 20], and visible light [21], have been used to follow the structural evolution on a macromolecular scale. The different scattering studies demonstrated that acid-catalyzed sols are linear and consisted of very little branching, whereas base-catalyzed sols have highly crosslinked structures [17, 18]. In addition, ^1H and ^{29}Si NMR [22–26], Raman [27, 28], and IR [26] have provided useful information on the molecular structure of the intermediates during the sol-gel process. Perhaps of greater importance is the structural development of the gel at the microscopic level. *In situ* monitoring of the sol-gel transition on a nanometer-scale has been accomplished by doping the sol-gel mixture with photochromic molecules [29–33]. A spectroscopically active molecule that is sensitive to its environment can serve as a structural probe during the evolution of the gel. There are a variety of photochemical compounds available that have a high sensitivity to matrix parameters such as polarity, viscosity, porosity, and local geometry.

The structural and chemical changes that transpire during the formation of an SiO_2 xerogel were monitored using spiropyrans by Levy and Avnir [29]. The mechanisms of the photochromic behavior of spiropyran dyes are well understood, making them useful compounds for analyzing the sol-gel process. A particularly useful characteristic of spiropyrans is that under certain conditions, they have "reversed photochromism" behavior. Reversed photochromism results when the stable form of the dye in the dark is the colored form, thus allowing it to be observed by bleaching it with UV irradiation. Levy and Avnir explained the changes they observed in the absorbance behavior of the spiropyran during the sol-gel transition as a gradual shift from solution behavior, where the dye is able to move freely within the matrix, to adsorption onto the silica surface, where the dye is immobile. Their conclusion was supported by previous studies that demonstrated how rotational isomerizations were restricted as an organic polymer grew due to the available "free volume" becoming smaller [34]. Early in the sol-gel process, the spiropyran was trapped in the pores containing the sol-gel solvent and was mobile; however, as the reaction proceeds, the matrix becomes more rigid and collapses around the spiropyran causing it to absorb onto the silica surface.

Additional evidence of adsorption of the spiropyran onto the surface was given by its reversed photochromism behavior during the gel-xerogel transition. It has been documented in the literature that molecules of the spiropyran family show reversed photochromism properties when adsorbed to silica [35–38].

A subtle change in the polarity of the pore solvent composition during the progression of sol-gel reactions has a significant influence on the photochromism-to-reversed photochromism characteristic. Initially, the pores are filled with the starting mixture of the silica alkoxide, water, and methanol. Once hydrolysis and condensation reactions begin, methanol and water are produced, and the pores become rich with aqueous methanol. Hydrolysis will cease while condensation continues, filling the pores with water only. Eventually, the water is evaporated and the gel is dried, leaving relatively few water molecules in the pores. The λ_{max} blue-shifts during the sol-gel transition, providing further evidence that the solvent environment of the pores changes from methanol to water.

This blue-shift was observed by de Mayo et al. [39]. The λ_{max} shifted from 545 to 498 nm when a spiropyran dye was in methanol and water/methanol mixture, respectively. The observations were attributed to a gradual shift in the dissolved spiropyran to adsorbed spiropyran equilibrium during the sol-xerogel transition.

The microscopic rigidity of tetraethoxysilane (TEOS) and mixed aluminosilicate (ASE) sol-gel systems were investigated by McKiernan et al. [30] using a rigidochromic molecule, a compound whose luminescence is dependent upon the rigidity of its surrounding medium. The TEOS and ASE mixtures were doped with bipyridyltriscarbonylchlororhenium(I), $ReCl(CO)_3bpy$, to monitor its emission spectrum during the sol-gel-solid transformation. The maximum emission wavelength, λ_{max}, of $ReCl(CO)_3bpy$ shifts to higher energy as the rigidity of its matrix increases. If the rigidity of the local environment changes enough to shift λ_{max}, the luminescence spectrum can be used to study the change in viscosity at the molecular level during the gelation procedure.

Reference values for λ_{max} of $ReCl(CO)_3bpy$, determined using liquid and solid (frozen) solvents, were used to calibrate the rigidochromic effect on the luminescence spectrum and then compared with values obtained during the sol-gel transition of the TEOS and ASE matrices. A blue-shift in the emission maximum was observed for pure ethanol and TEOS as they approached their respective freezing points, indicating that $ReCl(CO)_3bpy$ was sensitive to the rigidity of its environment and could be used for calibration purposes. They also determined that the emission maximum is independent of temperature in the sol-gel matrix over the 175 to 300 K range so that any spectroscopic shift observed during the sol-gel transition could be attributed to a change in the rigidity of the environment and not to a change in the temperature [30].

When $ReCl(CO)_3bpy$ was incorporated into the ASE mixture, the emission peak maximum remained constant during the formation of the sol and up to the gel point [30]. They attributed this behavior to the probe molecule not being constrained to the solid-phase oxide network, but instead, it was in a solvent-like environment. Their explanation was based on the comparison of the behavior of the $ReCl(CO)_3bpy$ when it was trapped in solid (frozen) solvents. The emission maximum was blue-shifted when solidification was accomplished by freezing, thus demonstrating that a macroscopic change in rigidity concurred with a molecular change in rigidity. However, when solidification was accomplished by gelation, a macroscopic change in rigidity was observed, but it was not accompanied by an increase in the rigidity of the microenvironment. At that stage in the process, the mobility of $ReCl(CO)_3bpy$ was not restricted and, therefore, behaved as a liquid. In contrast, the λ_{max} continually blue-shifted during the aging period until it stabilized at a value between the completely liquid phase and the completely solid phase. The microscopic environment became increasingly rigid during aging, and the probe molecule was no longer surrounded by the interstitial liquid phase, as it was during gelation. The local gel structure was drastically modified during aging, increasing the rigidity of the oxide skeleton. Furthermore, the gel structure collapsed and shrunk during the drying stage, progressively increasing the rigidity until complete rigidification was accomplished. This was supported by the additional blue shift in the emission spectra during the drying process. A final λ_{max} stabilized at the same value as that for the frozen solvent. It was concluded that the $ReCl(CO)_3bpy$ molecules were completely immobilized in the oxide network at that point.

The effect that the type of molecular precursor has on the rigidity of a solid made by a sol-gel process is demonstrated clearly when the above ASE system is compared to a tetraethylorthosilicate mixture [30]. The emission wavelength remained constant at a value close to that of the liquid during the sol formation, gelation, aging, and most of the drying stages. A blue shift was not observed until the solvent molecules were removed during the final drying period, indicating that the probe molecules were in a nonrigid environment throughout most of the sol-gel transition in the silica system.

By controlling the viscosity during gelation, the final product can be molded into the desired shape. For this reason, the sol-gel process is an attractive method for preparing solids. Viscosity depends on the size of the particles undergoing hydrolysis and condensation reactions. The larger the particles, the greater the viscosity. Therefore, any variable that causes the size of the molecules to increase also will increase the viscosity.

For related reasons, viscosity increases with reaction time. The assessment of the viscosity of materials produced by sol-gel processes on a microscopic level and the influence of the aging cycle on the reorientation dynamics of organic dopant molecules within these materials was reported recently by Narang et al. [32]. They investigated, by static and dynamic fluorescence spectroscopy, the local microviscosity surrounding a dopant molecule entrapped in a sol-gel mixture as a function of aging time and hydrolysis pH. Tetramethylorthosilicate (TMOS) based xerogels were doped with rhodamine 6G (R6G). Fluorescence anisotropic measurements were made periodically throughout the hydrolysis, gelation, aging, and drying stages. It was determined that the hydrolysis pH had no affect on the environment that R6G sensed; however, it did influence the kinetics of the sol-gel process. Evaluation of the steady-state fluorescence anisotropy measurements, which describe the average microviscosity surrounding a fluorescent probe, established that there were four distinct regions during the sol-gel transition: liquid-to-gel region, indicated by a gradual increase in anisotropy; aging region, indicated by a plateau in the anisotropy due to the continuation of polycondensation reactions and concomitant networking; initial stages of drying, represented by a rapid increase in the anisotropy due to the expulsion of solvent from the siloxane network and the collapse of the pores; and the dried gel region, denoted by a second plateau in the anisotropy due to a majority of the solvent being removed.

Time-resolved fluorescence anisotropic experiments were used to recover the rotational motions of a fluorescent probe in complex systems [32]. It revealed two rotational reorientation times for R6G during the sol-gel transition, indicating the existence of two domains with discrete microviscosities. One of the reorientation times remains constant (fast rotational reorientation time) and the other changes (longer rotational reorientation time) with aging time during the sol-gel process. The constant microdomain was assigned to R6G in a wet gel pore and the variable microdomain was assigned to R6G in a highly viscous environment. During the initial stages of the sol-gel process, the contribution to the total decay of anisotropy from the constant domain was high because the material was very porous, allowing R6G to rotate easily. However, its contribution decreased drastically as the process continued, as observed with an increase in the longer rotational reorientation time. It was concluded that dopant molecules were able to move during the sol-gel transition until the drying stage was reached.

Additional investigations of the above TMOS derived sol-gel were conducted using 6-propionyl-2-(dimethylamino)napthalene (PRODAN) as the dopant probe [33]. The emission properties of PRODAN are much more sensitive to changes in its microenvironment than R6G. The emission maxima remained constant well beyond the gel point, again demonstrating the microenvironment around the dopant molecule is unchanged through gelation. Furthermore, it was concluded that solvent was removed from the pores in a stepwise manner; first ethanol is expelled, followed by water. The mechanism of solvent removal was based on the red shift in the emission maxima that followed gelation, indicating a shift to a more polar environment. Finally, a distribution of time-resolved fluorescence lifetimes was observed after gelation, suggesting the existence of a heterogeneous microenvironment. Based on the steady-state and time-resolved fluorescence experiments, it was concluded that PRODAN was able to freely rotate even after the solid was dried under ambient conditions and the change in microviscosity was minimal until solvent was removed from the pores.

The aging step is crucial to the properties of importance in analytical chemistry of solids prepared by sol-gel processes. As demonstrated in the above examples, the polycondensation reactions continue long after the gel point is reached. The aging process, when carried out in the pore liquid matrix, can alter the structure of the gel further by increasing its rigidity and coarseness while reducing its size. Factors that affect the gel structure during the aging process are time, temperature, and pH. The effect of time was demonstrated by Iler et al. [40] who showed an increase in the strength of the gel (without changing the pore structure) and an increase in the coarseness (increasing the pore size while reducing the surface area through a dissolution and reprecipitation process) upon aging.

Increasing the temperature during the aging process influences the structure in two distinct stages [41]. The initial stages of wet aging result in dried gels that shrink less when they are aged longer, but there is an increase in their pore volume and diameter. Little change in the overall surface area is seen, however.

The time dependence of the aging process correlates to an increase in linkages which strengthens the gel, and results in less shrinkage during drying. The second stage leads to a decrease in surface areas, but the pore size continues to increase until eventually an insignificant change in the pore volume is reached.

Washing the gel to remove the liquid from the pores is also a type of aging. The pH of the wash solution can influence the final properties of the gel. For example, Girgis reported a decrease in surface area from 650 to 467 m^2/g while increasing the pore diameter when a silica gel was soaked at pH 10–11 for 1 day [42].

The physical properties of the gel change during aging because they are viscoelastic materials [43]; that is, they react to a stress in the system by taking on an instantaneous strain and a continuous viscous deformation. The rigidity and, therefore the gel strength, increases during aging. Furthermore, there is an increase in the elastic modulus and the viscosity. Overall, the aging process results in an irreversible decrease in surface area in conjunction with an increase in pore size.

In summary, recent studies show that the formation of solids by sol-gel chemistry is more complicated than suggested by early studies. Some of the important observations are in Table 1.

Overview of Analytical Methods Using Solids Prepared by Sol-Gel Chemistry

Spectrophotometric Methods

The ability to encapsulate a wide range of reagents in optically transparent matrices by sol-gel chemistry has been the basis of numerous reports of analytical methods. Optical methods of analysis have included both absorbance and fluorescence. There have been numerous recent reviews on this topic; among those which are especially informative are those by Lev and co-workers [44, 45] and by Dave et al. [46]. Hence, only a few examples are presented herein.

Lee and Saavedra [47] developed a sol-gel based pH sensor by employing the ability of these materials to encapsulate chemicals in a transparent matrix. Bromophenol blue was entrapped in a film prepared from tetraethylorthosilicate on a glass slide. The structure of this film prevented leaching of the dye yet was sufficiently porous to provide rapid exchange with hydronium ion. The resulting device responded

Table 1. Selected examples of characterization of sol-gel chemistry

Observation	Method	Ref.
Gradual shift from dissolved to adsorbed equilibrium of dopant molecule during sol-gel transition	photochromism	29
Change in the polarity of the pore solvent due to the pore environment shifting from alcoholic aqueous during sol-gel transition	photochromism fluorescence anisotropy	29, 33
Solution-like behavior of probe molecule from the initial formation of the sol until the gel point (aluminosilicate)	rigidochromism	30
Macroscopic and microscopic environment becoming increasingly rigid during aging, and complete rigidification occurs during drying (silica)	rigidochromism	30
Microscopic rigidity remains constant during the sol-gel process until the final drying stage is reached	rigidochromism fluorescence anisotropy	30 33
Four stages during the sol-gel transition: liquid-to-gel, aging, initial drying, dried gel	steady-state fluorescence anisotropy	32
Two discrete domains of microviscosity exist during the sol-gel transition: one constant and the other variable	time-resolved fluorescence anisotropy	32, 33

rapidly to pH change. The acid-base chemistry of bromophenol blue was monitored by attenuated total reflectance of 457.9 nm light. A useful response to pH over the range 3–6 was observed even one year after fabrication (with the device stored dry except during measurements). It is interesting to note that the apparent pK of the dye changed with time. Three months after preparation the pK was 4.5 rather than the value of 4.1 that is characteristic of this dye in aqueous solution; after one year the value was 5.2. This illustrates the structural effect of the xerogel on the optical spectroscopy. As noted earlier, the xerogels do not provide a stable microenvironment but instead continue to shrink as they age under ambient conditions.

A fluorescence-based determination of Fe(III) using a reagent entrapped in a material prepared by the sol-gel process was reported by Barrero et al. [48]. Pyoverdin, which is a natural fluorescent pigment, was added to the tetramethylorthosilicate from which the xerogel was prepared. It was dried under ambient conditions for two weeks followed by overnight treatment under vacuum to remove residual liquid. A flow cell was used to establish that pyoverdin was not leached into test solutions over the pH range 3–9. The doped xerogel was stable over a 12-month period. Fluorescence quenching by Fe(III) was observed; a calibration curve was linear over the range 3–300 ng Fe/mL (correlation coefficient, 0.997). The relative standard deviation of 10 replicates of a 150 ng Fe/mL sample was 3%. Perhaps the most important observation was that the stability was far superior to a comparable sensor prepared by immobilizing pyoverdin in a controlled pore glass.

Potential problems in using sol-gel chemistry to support fluorescent probes were elucidated by Narang et al. [49]. A synthetic organic receptor, dansyl-glycine-β-cyclodextrin, which exhibits fluorescence, was immobilized by adding it to a tetramethylorthosilicate solution prior to formation of a spin-cast solid film. Three important positive results were shown. First, the presence of borneol was illustrated to decrease the fluorescence, thereby potentially serving as the basis for an analytical procedure. Second, this dansyl probe in the solid film was shown to function reversibly; this was accomplished by a scheme involving a rinse with ethanol. Third, the mechanism of action was demonstrated to be expulsion of dansyl from the cyclodextrin cavity by borneol rather than just fluorescence quenching by borneol. An important problem, related to the aging of the film, was that the sensitivity toward borneol decreased with time. After three weeks a response was not observed.

There are two likely causes of this effect of age on the response, namely, expulsion of the solvent and decrease in the mean pore diameter with time [49]. The results suggested that the latter was the more significant with this system. Two strategies to provide greater lifetimes were explored. The sol-gel (a viscous liquid) was aged four weeks before the film was cast, and base-catalysis of the formation of the silica network was used to increase the pore size. The former did not improve the stability, and the latter procedure was not compatible with retaining fluorescence of the probe due to cleavage of the ether between dansyl and the cyclodextrin. This result is consistent with citations in the previous section on the influence of aging on the spectroscopy of compounds immobilized by the sol-gel process. Although some workers have reported long term stability of spectroscopic sensors prepared by sol-gel processes, the influence of age on such media suggests that it cannot be assumed that procedures taken from liquid phase studies will work when the reagents are immobilized in xerogels and related materials.

Browne et al. [50] coated fiber optic waveguides with doped films prepared by a sol-gel process as a means of developing chemical sensors. A pH-induced shift in the absorption spectrum of fluorescein in a silica xerogel was used as the basis of a pH sensor. An aluminosilica-based system had sufficiently large pore sizes to allow detection of a quinone, quinizarin, but the time required to obtain the maximum signal was 30 min. It is important to note that the authors were cognizant of the potential problems related to aging of xerogels on fluorescence spectra; they suggested that use of a kinetic method (fluorophore decay kinetics) to quantify the results can reduce problems related to structural changes and to leaching of the fluorophore.

Fiber optics that were coated by the sol-gel process also were used in fluorescence-based sensors for oxygen [51, 52]. Here, quenching of the fluorescence of a $\mathrm{Ru^{II}}$(diphenyl-1,10-phenanthroline) complex provided the readout that was related to the partial pressure of O_2. The actual measurements were either by phase fluorimetry (which relates to the fluorescence decay kinetics) [51] or by direct luminescence [52].

Dunbar et al. [53] reported what is perhaps the most thorough evaluation of sol-gel based sensors. Using the quenching of pyrene fluorescence by oxygen as a probe, the influence of age on the optical spectroscopic behavior of films prepared by a sol-gel process was investigated. Both static and time-resolved fluorescence measurements were employed in the study. The silica films were prepared by controlled dip-coating of a fiber optic into hydrolyzed tetramethylorthosilicate or tetraethylorthosilicate that was doped with pyrene. As discussed below, the doping procedure had a significant influence on the behavior. The fluorescence measurements were made in the presence and absence of oxygen over a period of one year. Even though the film appeared to be dry within a few minutes, the behavior varied markedly with time for one month, after which the change was slower but still significant.

The importance of the microenvironment of pyrene in the solid was demonstrated [53]. Analysis of the spectroscopic behavior of pyrene in the film relative to that in various liquids suggested that the microenvironment of the solid is "apparently alcohol-like", suggesting an influence of residual silanol groups within the xerogel. The average life-time of excited states of pyrene within the xerogel decreased with aging of the film. The nature of the microenvironment depended upon the time that the tetramethylorthosilicate was hydrolyzed prior to doping with the pyrene (note that the doping, which was done after 1–5 days of hydrolysis, is still into a liquid-like matrix; solidification occurs at longer times or after preparing a thin coating). Longer fluorescence lifetimes were achieved with doping after one day of hydrolysis than after five days. It is important to note that very poor results were obtained when the pyrene was added prior to initiating the hydrolysis. The difference between "one day" and "five day" films persisted over the entire aging period. They also found that overall performance of these fluorescence-based sensors was better with the tetraethyl than with the tetramethyl orthosilicate as the precursor in terms of the relative decrease in quenching rate. The greatest stability is obtained with films aged for 1–2 months [53].

Bioanalytical Methods Employing Optical Readout

The use of the sol-gel process in the design of biosensors clearly is the most common analytical application of this chemistry. The attractive feature of this approach is the potential to immobilize an enzyme without compromising its aqueous solution selectivity and activity. A related feature is the ability to encapsulate enzymes or other proteins in a manner that prevents them from leaching into solution while retaining pathways of substrates and co-factors to the reactive site. Moreover, the reaction products in the matrices formed by sol-gel chemistry can be interrogated by both electrochemical and spectroscopic methods, which are the measurement strategies that are most commonly employed in biosensors. Avnir et al. [54] have reviewed the encapsulation of organic molecules, including enzymes, and previously cited reviews [44–46] also addressed biosensors.

The initial reports of both optical and amperometric sol-gel biosensors used glucose as the analyte. Yamanaka et al. [55] used optical measurements to monitor the hydrogen peroxide formed from an enzymatic reaction of glucose. Here, glucose oxidase and horseradish peroxidase (HPR) were both immobilized in silica by a sol-gel process. Also included were 4-aminoantipyrine and *p*-hydroxybenzene sulfonate, which served as precursors of a dye formed by an HPR-catalyzed reaction involving hydrogen peroxide. The overall result was the formation of a dye with an absorbance maximum at 510 nm when the doped silica monolith was exposed to glucose.

To circumvent problems related to dye formation as the signal-generating reaction in a sol-gel based biosensor [55], Yamanaka et al. [56] doped silica with the phosphate ester of nicotinamide adenine dinucleotide, NADP, which functions in silica as a coenzyme for dehydrogenase reactions. The fluorescence spectrum of NADPH was used to monitor the enzymatic reactions. The emission intensity varied with the concentration of a substrate, D-glucose-6-phosphate, over the range 3.3–39 mM. By comparing the behaviors in aged and dried sol-gel materials, it was concluded that encapsulation in silica monoliths slowed the turnover rate.

Blyth et al. [57] encapsulated metalloproteins in silica in the study of sensors for NO and CO. The basic chemistry of redox of metalloproteins in silica was investigated, a key point of which was the demonstration of reversible reduction of Fe(III) centers in hemoglobin, myoglobin, and cytochrome *c* by dithionite. In a 1.5 mm film of silica, the reduction was complete within 15 min with all three proteins. With NO as a reactant, binding was observed with immobilized cytochrome *c* when iron was in the oxidized form but not when it was in the reduced form, whereas it bound to both the oxidized and reduced states of the other two proteins. With CO as the reactant, reaction was observed only with Fe^{II} in hemoglobin and myoglobin; reaction with cytochrome *c* required denaturing the protein. That reversible binding and color changes upon binding were found allowed the projection of this chemistry to the design of biosensors; however, only preliminary semiquantitative results were presented.

Encapsulation of myoglobin (Mb) in silica by sol-gel chemistry was employed by Chung et al. in a sensor for dissolved oxygen [58]. Reduction to deoxy-Mb was accomplished with dithionite. Upon exposure of the doped silica to an aqueous solution containing dissolved oxygen, oxy-Mb was formed in a quantity related to the concentration of oxygen in the solution. This conversion resulted in a change in the absorption spectrum over the region *ca.* 400–460 nm; measurement at 431.5 nm was suited to monitoring the dissolved oxygen concentration. The mechanism of signal generation suggests possible utility as a sensor. However, calibration data were obtained only over the range 20–100% saturation, and chemical reduction was necessary to generate the sensor.

While these results show the potential utility of optical biosensors based on sol-gel chemistry, the emphasis has been on the attractiveness of immobilizing enzymes by this procedure rather than systematic analytical investigations, including comparison to related devices. Pragmatic problems related to regeneration of baselines and optimizing response times and sensitivities may limit their utility. As indicated by the studies in the previous section, long term stability, especially if fluorescence is used as the monitoring process, may also be a problem. Selected examples of spectroscopic methods using sol-gel chemistry are shown in Table 2. Also included are some observations related to analytical method development.

Table 2. Selected analytical studies using spectroscopic measurements on matrices prepared by sol-gel chemistry

Analyte/observation	Ref.
Fe(III) determination by quenching of pyoverdin fluorescence	47
Influence of aging of a xerogel on the fluorescence of an encapsulated reagent	48, 52
Role of residual groups of silica on fluorescence of encapsulated pyrene	52
Optical biosensor for glucose	54
Optical biosensors for NO and CO	56
Optical biosensors for dissolved oxygen based on spectrophotometry of myoglobin	57

Chromatographic Supports Prepared by Sol-Gel Chemistry

The ability to synthesize highly porous solids in a manner with controlled pore sizes by sol-gel chemistry suggests that this chemistry is suited to the development of stationary phases for gas and liquid chromatography. The merits of controlled porosity glass as a stationary phase have been demonstrated in a study which employed conventional thermal methods of synthesis along with leaching to prepare the material [59]. That particles of selected sizes, monoliths of controlled porosity, and films of constant thickness can be prepared by sol-gel chemistry increases the scope of possible application. Indeed, there have been some applications of this chemistry to chromatography reported.

Fields [60] developed a high-performance liquid chromatographic column with a continuous silica xerogel as the stationary phase. The primary characteristic of the xerogel was a mean pore diameter of 2 μm and a range of 0.2 to 3 μm. Columns longer than 20 cm had voids in the range of 0.1–1 mm that were observed visually. Using an acetonitrile/water mixture of 95/5 (v/v%) as the mobile phase, back pressures ranged from 23 psi at 0.5 μL/min to 632 psi at 10 μL/min when the column geometry was on the order of 0.3 mm i.d. and 15 cm length. These values were lower than those obtained with a comparable column geometry but with 5 μm spherical silica particles as the packing material and compared favorably to back pressures reported for continuous columns with organic polymers as the support. The column efficiency was 5000 plates/m for ethyl benzoate (capacity factor, 0.8) and 1.3×10^4 plates/m for naphthalene (capacity factor, 2.0) at 0.5 μL/min.

Further use of sol-gel chemistry in chromatography can be anticipated. For example, the combination of continuous supports in conjunction with on-column detection has potential applicability due to the optical characteristics of silica xerogels.

Applications of Sol-Gel Processes to Electrochemistry

Certain solids prepared by sol-gel chemistry exhibit electronic or ionic conductivity. Such materials have found extensive application in the design of electrochromic devices, as supports for electrocatalysts, and in the development of fuel cell electrodes. An overview of this topic is provided by Dunn et al. [61]. Selected examples will be presented herein.

To date, these materials have been used rarely in electroanalytical methodology. Most of the reported applications to electroanalytical chemistry have involved amperometric monitors for biosensors, as described below. Also summarized are other uses of conventional voltammetric methods in studies using solid electrolytes prepared by sol-gel chemistry.

Electrochromic Devices

Materials which have oxidation states with markedly different absorbance spectra in the visible region can serve as electrochromic devices. For example, WO_3, which is among the most commonly studied electrochromic material, changes from an initial light yellow-to-colorless state to a dark blue material upon partial reduction of the solid. This property was exploited in solid-state electrochemical cells such as adjacent thin films of WO_3 with a transparent ionic conductor (such as a lithiated conducting polymer) sandwiched between conducting glass plates [62]. Sol-gel chemistry is being explored as a means of depositing the electrochromic layer [62–64].

The efficiency of WO_3 as an electrochromic device is influenced by inclusion of TiO_2 in the solid matrix [63]. An increase in the titanium content leads to greater stability in terms of reproducibility of the coloration-bleaching cycles over time. Homogeneous mixtures can be obtained by preparing the solid by sol-gel chemistry from a solution containing WCl_6 and tetraisobutyl orthotitanate [63]. Cyclic voltammetry ($0.5\,M$ $LiClO_4$ in γ-butyroacetone) was performed on films prepared by sol-gel chemistry and by sputtering. In both cases, the Ti content was varied. Reduction of WO_3 was observed over a broad potential range with the onset of the process at about -0.5 V *v.* Ag/AgCl, and oxidation yielded a peak at about -0.4 V. The magnitude of the current decreased with the addition of titanium. Indeed, the intensity of the coloration of the Ti-containing films also was lower than that observed with pure WO_3 [63].

While Göttsche et al. [63] did not remark on any major difference in behavior of sputtered and sol-gel films of WO_3, Bell et al. found that the switching speed of sol-gel based electrochromic devices was slower than that for other types in the literature [62]. But perhaps their most important observations in terms of possible electroanalytical applications of solids prepared by sol-gel processes related to the differences in charge-transfer through films prepared by different precursors [62]. Here, WO_3 films were deposited from ethoxide and butoxide precursor solutions. Cyclic voltammetry of these films in $1\,M$ $LiClO_4$ solutions in dry propylene carbonate showed lower current densities with the latter as the precursor. The films prepared from butoxide were significantly rougher, as shown by atomic force microscopic measurements on films that were fired at 300 °C for 30 min. Also, the films had different mechanisms of coloration.

Macêdo and Aegerter [64] employed a variety of sol-gel processes in the design of an electrochromic device. Three layers, all of which were made by sol-gel chemistry, were sandwiched between plates of indium tin oxide glass. The ion-conducting layer was a mixture of CeO_2 and TiO_2; current-time curves obtained by double potential step chronoamperometry (± 1.5 V applied) were stable for up to 3×10^4 cycles. The color-forming layer contained WO_3 mixed with TiO_2; the optical behavior (color-bleaching cycles) was stated as comparable to that observed with other methods of preparation but with a shorter lifetime. The authors stated that the components of this device may find more application in battery design than in an electrochromic device. Indeed, this may generally be true of sol-gel based films that have been tested to date for electrochromic devices.

Electrodes for Batteries, Fuel Cells, and General Electrochemistry

Much of the interest in preparing electrodes by sol-gel chemistry involves the possibility of making rechargeable cathodes. This can be illustrated with the example of the electrochemistry of vanadia films in propylene carbonate containing $LiClO_4$ as the supporting electrolyte. The xerogel, $V_2O_5 \cdot nH_2O$, is formed from a sodium vanadate solution by replacement of sodium with proton by ion-exchange to yield vanadic acid, which spontaneously undergoes polycondensation with loss of water to form a viscous gel [65]. Further aging forms the xerogel, a process that is rapid when thin films are cast from the viscous material. Imposition of a cathodic current results in an electrode voltage in the range 2 to 3.2 V *v.* a Li^+/Li

electrode; V(V) is partially reduced with the concomitant intercalation of Li^+ into the xerogel film [66]. The utility of the vanadia xerogel as a battery cathode was limited because lower current densities were obtained than with polycrystalline material. However, a mixture of 20% graphite and 80% vanadia showed higher conductivity and a greater ability to retain current capacity with repeated recharges [66]. A vanadia aerogel (prepared by supercritical drying of the xerogel with CO_2) that was mixed with carbon and pressed into a nickel screen was evaluated as a cathode in contact with an electrolyte of 1 *M* $LiClO_4$ in propylene carbonate [67]; the behavior was similar to that of the xerogel [68].

We can envision analytical application of these electrodes growing in importance, especially because high current capacity is not as important in electroanalytical chemistry as in energy sources. One of the possible applications would involve using the partially reduced films of vanadia as an electron transfer mediator.

The above reports are typical of a variety of studies in which the nature of the xerogel and/or the intercalated cation is varied. A recent report on the intercalation of Li^+ into $Al_{0.11}V_2O_{5.15}$ contains a summary of several such studies [69].

An important investigation of the general electrochemical properties of coatings made by sol-gel chemistry was that by Ŝtangar et al. [70]. The cyclic voltammetry of xerogels that had Ce(IV) incorporated into the backbone was reported. The indicator electrode was indium tin oxide that was coated with either a ceria or a mixed ceria-titania xerogel, and the supporting electrolyte was 0.1 *M* LiOH. In freshly prepared xerogels, the former yielded higher reversibility which reflects the relative ease of Li^+ intercalation into the film. Aging improved the behavior of the mixed ceria-titania xerogel in this regard. In all cases the reduction of Ce(IV) was observed at about −0.8 V *v.* Ag/AgCl. Thicker films yielded higher currents and more negative peak potentials.

A significant observation was that annealing the films was not deleterious to the electrochemical behavior except for a diminution of current by about a factor of two [70]. Cyclic voltammetry at electrodes annealed at 500 °C yielded cathodic and anodic peak potentials at *ca.* −0.8 and −0.2 V, respectively, whereas the corresponding values were −0.6 and −0.2 V with an annealing temperature of 300 °C. The film thickness decreased from 57 to 48 nm when the higher annealing temperature was used. The general voltammetric behavior was investigated in this paper in terms of these films serving as a counter electrode for electrochromic devices, but our view is that they may be well-suited to serve as electron-transfer mediators or catalysts for electroanalytical applications as well.

The preparation of electrocatalysts by sol-gel chemistry has been the goal of several reports. Mixed RuO_2-TiO_2 systems have been studied frequently, perhaps because of the well-known efficacy of the thermal oxide of ruthenium on a titanium support as a catalyst for electrocatalytic chlorine production. Guglielmi et al. [71] described a variety of synthetic procedures for making these mixtures, but electrocatalytic studies were not performed. The electrochemical activity of Ru-Ti mixtures prepared by conventional and sol-gel procedures was compared by Hwang et al. [72]. Perhaps because the latter results in a more porous structure, it provided a greater population of active sites and charge capacity. Cyclic voltammetry in 1 *M* NaCl at pH 2 did not yield well-developed current-voltage curves, however.

In a related study, El Baydi et al. [73] used the sol-gel process to obtain a more porous structure of a Co_3O_4 electrocatalyst than obtained by a conventional method. Cyclic voltammetry in 1 *M* KOH showed a well-defined pair of peaks for the Co(IV, III) couple just prior to the oxygen evolution reaction. It is interesting to note that the electrode could not be made by simply dip-coating of the gel onto a conductive material. Instead, the powdered solid was mixed with isopropanol and "painted" onto a polyisobutylene foil that contained graphite to provide conductivity.

In summary, sol-gel chemistry clearly is suited for the preparation of electrocatalysts. Whether these materials will lead to improved analytical methodology is a question that is only just beginning to be explored.

Electroanalytical Methods Employing Sol-Gel Chemistry

As suggested above, few actual applications of sol-gel chemistry to electroanalysis have appeared. Most applications have used amperometry as a monitor for enzymatic reactions in biosensors or in flow injection systems, the basis of which is the assertion that enzymes in materials prepared by sol-gel chemistry have behaviors closely related to their chemistry in water but are strongly bound in terms of resistance to leaching into a contacting liquid. This hypothesis was developed using optical probes of enzyme activity.

To extend the scope of such characterization studies to materials that are not suited for optical measurement, Audebert et al. used electrochemical methods to monitor enzyme activity [74]. Glucose oxidase and a ferrocene compound were immobilized in different types of silica in a hemispherical coating on a glassy carbon electrode. The modified electrode was placed in an aqueous phosphate buffer that was saturated with the ferrocene, and cyclic voltammograms were obtained in the presence and absence of glucose. The reversible redox of ferrocene was observed; the peak potential difference appeared to be less than 100 mV. In the presence of $0.1\,M$ glucose, a voltammogram obtained after about 20 min showed an increase in the anodic current and a decrease in the cathodic current which is diagnostic for a mediated reaction. The current increase was (nonlinearly) related to glucose concentration up to $1\,M$.

That this method for immobilizing enzymes was suited to quantitative determinations of glucose by amperometry was better-shown by Tatsu et al. [75]. Here, glucose oxidase that was encapsulated in silica was used in conjunction with an amperometric oxygen electrode to monitor glucose in a flow injection system. The current-time curve developed when glucose was injected was integrated, and the charge obtained was plotted *v.* glucose concentration. The calibration curve extended from about 20–400 mg glucose/dL. The glucose oxidase activity was retained for at least 2 months during storage in a desiccator at 4 °C. Although this analytical scheme does not have the stand-alone characteristic of a sensor, the results suggest the development of an amperometric biosensor for glucose.

Glezer and Lev [76] developed an amperometric glucose biosensor that employed a sol-gel process to encapsulate glucose oxidase in vanadia. A platinum electrode was dip-coated with an enzyme-containing gel. Upon drying, this film-coated electrode was used as the indicator in a three-electrode voltammetric cell. Cyclic voltammetry of buffered, glucose-containing solutions showed a current-voltage for the oxidation of hydrogen peroxide; the magnitude of the current was related to the concentration of glucose.

Pankratov and Lev [77] made a composite of organically modified silica and carbon which was subsequently used to develop a new amperometric biosensor for glucose. The sensor had several interesting features. An organically modified surface was used to minimize penetration of water into the bulk of the silica. Inclusion of carbon powder increased the conductivity of the composite. Third, an investigation of the influence of a mediator, tetrathiafulvalene (TTF), on the performance of the sensor was performed. The presence of TTF allowed the monitoring of glucose oxidation at a potential more than 500 mV lower than that when hydrogen peroxide is the product, and with the TTF mediator, the response was independent of O_2 level (the expected result). Steady-state currents were developed in 30–100 s in the presence of TTF, and this current was not influenced by stirring the solution. It also was noted that the composites were sufficiently brittle to allow mechanical polishing to renew the surfaces.

Sampath and Lev recently described a somewhat different composite as an electrode for an amperometric biosensor [78]. Here, the main change was using Pd rather than TTF as the mediator. The purpose was to employ Pd as the electrocatalyst for the oxidation of hydrogen peroxide which is produced by the oxygen-mediated oxidation of glucose in the presence of glucose oxidase. The Pd lowered the overpotential for the oxidation of hydrogen peroxide in the carbon-containing composite by about 400 mV. This catalyst was obtained by including $PdCl_2$ in the solution used to prepare the xerogel and reducing Pd^{2+} to Pd with H_2.

The organically modified silica composite with carbon [78] had other important features. The signal for 5 mM glucose was constant during a continuous, six-hour experiment (after which time the trial was terminated). The porous structure of the silica was exploited to allow entry of oxygen to the composite from the side not exposed to the sample, thereby suggesting a strategy for alleviating the problem of limited oxygen activity in some samples. The thickness of the reaction layer was adjusted by inclusion of hydrophobic components. The measurement strategy was extended to lactate and phenylalanine by incorporating lactate oxidase and L-amino acid oxidase, respectively.

Another novel approach to employing the sol-gel process in electroanalytical chemistry was to use enzymes encapsulated by this chemistry in a carbon ink suited to the fabrication of sensors by screen-printing methodology [79]. Glucose sensors that respond in about 10 s, are stable for about three months, are linear over at least the range 2–20 mM glucose, and have sensitivities on the order of 300 nA/mM for a 1.5% glucose oxidase content were made. The repeatability of current measurements made with a 2 mM glucose sample was 588 nA with an 11% relative standard deviation (10 different electrodes).

Dave et al. monitored the hydrogen peroxide and ethanol in porous materials prepared by sol-gel processes, reportedly on the basis of mediation of electron transport across the solid by $Fe(CN)_6^{4-,3-}$ [80]. A nearly linear current-voltage plot was obtained when a monolith between a pair of gold electrodes comprised the cell. In the presence of ethanol vapors and encapsulated alcohol dehydrogenase, voltammetry that is consistent with the well-known case of mixed-valence, solid state voltammetry with two polarizable electrodes [81, 82] was seen. Specifically, peak-shaped current-voltage curves that are symmetric around zero volts were developed. Consistent with the formation of mixed oxidation states as a result of mediating the enzymatic reaction, this "bioamperometric" current was related to the amount of ethanol vapor, so the device constitutes a gas-phase amperometric biosensor. A noteworthy difference between this and the above-cited electroanalytical systems is that a contacting liquid phase is absent in this case.

Dulebohn et al. [83] have investigated an approach to development of an electrochemical CO sensor in which a Rh(I) complex was encapsulated in zirconia and titania films. A cyclic voltammogram of a film-modified Pt electrode contacted to $0.1M$ $LiCF_3SO_3$ in water showed a peak that was related to exposure to CO. An important feature was that a subsequent purge of the cell with nitrogen resulted in the original baseline voltammogram in about 10 min. A quantitative relationship was not reported.

A potentiometric sensor for CO_2 was reported in which the active element was sodium super-ionic conductor (NASICON) [84]. Unlike other studies with NASICON, the material in this study was prepared by a sol-gel process. The gel was made from alkoxides of Si, Zr, P, and Na; dried at 90 °C for 20 h to yield a powder; pressed into a disk; and sintered at 900–1100° for 50 h. The 90% response time was less than 10 s at an operating temperature of 300–400 °C.

A potentiometric sensor for Na^+ in solution was prepared by incorporating a neutral carrier in a xerogel [84]. The response mechanism was as a ion-sensitive field effect transistor. The sensor responded to Na^+ over the range $10^{-6} - 1M$ and had a selectivity over K^+ of 6×10^{-3}.

An electrode modified by a sol-gel process was shown to exhibit permselective preconcentration by ion-exchange [86]. The sensitivity for the voltammetric response to $Fe(CN)_6^{3-}$ was increased by a factor of 8 due to preconcentration of this anion for 10 min whereas it suppressed the sensitivity toward $Ru(NH_3)_6^{3+}$ and the methyl viologen dication. Here, the film prepared by a sol-gel process contained an amine functionality. A carboxylate functionality was used when a residual cation-exchange capacity was the objective.

We have investigated dried gels as matrices for both general electrocatalysis and for amperometric sensor supports. In our work we have emphasized solid-state voltammetry; that is, electrochemistry by conventional techniques but performed in the absence of a contacting liquid phase. This field dates to the early 1960s if development of electrodes for fuel cells and batteries is considered; however, such studies are not as concerned with the precise interaction of current, potential, and concentration that characterizes electroanalytical chemistry. Analytical solid-state voltammetry, which requires such control, is a quite new field.

Our primary reason for considering sol-gel processes is the possibility that solid-state amperometric sensors for gaseous analytes which show little dependence on humidity may be developed. Previous reports on such sensors generally have employed Nafion®, a perfluorinated polymer with sulfonate functionality, as the solid electrolyte. For example, Yasuda et al. [87] developed a Nafion-based solid-state amperometric sensor for CO and presented calibration data (current *v.* concentration at 20 °C and 60% relative humidity) over the range 25–2000 ppm CO in air; however, a linear dependence of response of such sensors with relative humidity has been reported [88].

There is some evidence that certain solids prepared by sol-gel chemistry may yield voltammetric responses with limited influence of humidity. Once such indication is the data presented by Oliver et al. on the voltammetry of a ferrocene compound in a gelling mixture of tetraethylorthosilicate, water, the test compound, and an acidic catalyst [89]. Cyclic voltammograms were obtained over a period of time corresponding to the drying of the gel. Over a wide range of water content, the peak currents stayed constant.

We have tested a hypothesis based on the above report that addition of water to a xerogel doped with an electrochemically active couple will not influence the voltammmetric response over a wide range. A vanadia xerogel was doped with $Fe(phen)_3^{2+}$, where phen is 1,10-phenanthroline, and cyclic voltammetry over a range of scan rates was performed [90]. The xerogel was in the form of a thin film over an interdigitated microelectrode array, and the coated array was surrounded by argon during the experiments. After each set of experiments, small amounts of water were added to the solid electrolyte. In the range 100–1000 mV/s, the anodic peak current was proportional to the square root of scan rate, indicating a mass transport limited current, and at the slow scan rates, the current approached independence of scan rate, indicating semi-hemispherical mass transport to an ultramicroelectrode. This behavior, which emulates the voltammetry in simple liquid phases, is evidence of the utility of solids prepared by sol-gel chemistry as supporting electrolytes for electroanalytical chemistry, even when a contacting liquid phase is not present. Moreover, a range of rehydration level was found over which voltammetric peak currents were constant, an observation that supports the above hypothesis. It should be noted that the rehydrated xerogel was still rigid with no evidence of a bulk liquid phase; microphase water in the form of a liquid in the pores of the solid certainly exists, however.

Using a vanadia xerogel as the solid-state electrolyte and an indicator electrode that was modified with a thin film of a mixed-valence ruthenium oxide catalyst, we demonstrated that an anodic process in the presence of ammonia vapors was developed [90]. Subsequently, it was shown to be the oxidation of ammonia [91]. A linear calibration curve (current *v.* ammonia concentration in an argon atmosphere) was obtained under potentiostatic conditions over the range 2–27 μmol/mL. In a later study, the xerogel was doped with a solid-state buffer, maleic acid/hydrogen maleate, which held the pH near 2 (assuming that the solid-state pK is near that in aqueous solution) when the solution was exposed to ammonia vapors. Using the buffered xerogel increased the sensitivity of the ammonia sensor by a factor of 40 [92].

In summary, using sol-gel processes to immobilize enzymes presently is the primary reason for the growing use of this methodology in electroanalytical chemistry. However, the resulting solid has other attractive features, especially relative to the extensively studied organic polymers as electrode modifiers and as solid-state electrolytes for gas analysis. The gels can host dopants by a wider variety of mechanisms than organic polymers. The latter typically are used only as ion-exchangers or ultrafilters when used to modify electrodes. The gels are highly porous, so small molecules can readily diffuse in these materials. The presence of pore water imparts the general characteristics of aqueous solution chemistry to the gels; however, these materials are rigid and physically stable. A major disadvantage is the penchant for fracturing when the gels are contacted to liquids. This is especially true if the drying stage is too fast and/or if monoliths rather than thin films are employed. Using them as electrolytes for solid-state electrochemistry of gaseous species may, therefore, be the most common application in the near future.

Acknowledgment. This work was supported in part by the donors to the Petroleum Research Foundation administered by the American Chemical Society through Grant 26538-AC5.

References

[1] M. Ebelman, *Ann. Chimie Phys.* **1846**, *16*, 129.
[2] T. Graham, *J. Chem. Soc.* **1864**, *17*, 318.
[3] C. B. Hurd, *Chem. Rev.* **1938**, *22*, 403
[4] R. Roy, *J. Am. Ceram. Soc.* **1956**, *39* 145.
[5] R. Roy, *J. Am. Ceram. Soc.* **1969**, *52*, 344.
[6] R. K. Iler, in: *The Chemistry of Silica*, Wiley, New York, 1955.
[7] W. Stober, A. Fink, E. Bohn, *J. Colloid Interface Sci.* **1968**, *26*, 62.
[8] L. Levene, I. M. Thomas, U. S. Patent 3,640,093 (February 8, 1972).
[9] H. Dislich, *Angewandt Chemie* **1971**, *10*, 363.
[10] B. E. Yoldas, *J. Mater. Sci.* **1975**, *10*, 1856,
[11] B. E. Yoldas, *J. Mater. Sci.* **1977**, *12*, 1203.
[12] M. Yamane, A. Shinji, T. Sakaino, *J. Mater. Sci.* **1978**, *13*, 865.
[13] A. Aelion, A. Loebel, F. Eirich, *J. Am. Chem. Soc.* **1950**, *72*, 5702.
[14] H. Schmidt, A. Kaiser, M. Rudolph, A. Lentz, in: *Science of Ceramic Chemical Processing* (L. L. Hench, D. R. Ulrich, eds.), Wiley, New York, 1986, p. 87.
[15] H. Schmidt, H. Scholze, in: *Glass, Current Issues* (A. F. Wright, A. F. Dupuy, eds.), Martinus Nijhoff, Dordrecht, 1985, p. 253.
[16] H. Schmidt, A. Kaiser, *Glastechn. Ber.* **1981**, *54*, 338.
[17] C. J. Brinker, K. D. Keefer, D. W. Schaefer, C. S. Ashley, *J. Non-Cryst. Solids* **1982**, *48*, 47.
[18] C. J. Brinker, K. D. Keefer, D. W. Schaefer, R. A. Assink, B. D. Kay, C. S. Ashley, *J. Non-Cryst. Solids* **1984**, *63*, 45.

[19] K. A. Hardman-Rhyne, T. D. Coyle, E. P. Lewis, *Presented at the 1983 Annual Meeting of the Canadian Ceramic Society, Montreal, Quebec, February, 20–23, 1983.*

[20] J. Kjems, T. Freltoft, *Adv. Solid State Phys.* **1985**, *25*, 669.

[21] A. J. Hunt, P. Berdahl, *Mater. Res. Soc. Symp. Proc.* **1984**, *32*, 275.

[22] W. G. Klemperer, V. V. Mainz, D. M. Millar, in: *Better Ceramics Through Chemistry II* (C. J. Brinker, D. E. Clark, D. R. Ulrich, eds.), Mat. Res. Soc., Pittsburgh, PA, 1986 p. 3.

[23] W. G. Klemperer, V. V. Mainz, D. M. Millar, in: *Better Ceramics Through Chemistry II* (C. J. Brinker, D. E. Clark, D. R. Ulrich, eds.), Mat. Res. Soc., Pittsburgh, PA, 1986 p. 15.

[24] D. H. Doughty, R. A. Assink, B. D. Kay, in: *Silicon-Based Polymer Science: A Comprehensive Resource* (J. M. Zeigler, F. W. Gordon Fearon, eds.), *Advances in Chemistry Series No. 224*, American Chemical Society, Washington, D. C., 1990, pp. 242–250.

[25] H. D. Marsmann, E. Meyer, M. Vongehr, E. F. Weber, *Macromol. Chem.* **1983**, *184*, 1817.

[26] C. C. Lin, J. D. Basil, in: *Better Ceramics Through Chemistry II* (C. J. Brinker, D. E. Clark, D. R. Ulrich, eds.), Mat. Res. Soc., Pittsburgh, PA, 1986, p. 585.

[27] J. L. Lippert, S. B. Melpolder, L. W. Kelts, *J. Non-Cryst. Solids* **1988**, *104*, 139.

[28] C. A. M. Mulder, A. A. J. M. Damen, *J. Non-Cryst. Solids* **1987**, *93*, 169.

[29] D. Levy, D. Avnir, *J. Phys. Chem.* **1988**, *92*, 4734.

[30] J. McKiernan, J. C. Pouxviel, B. Dunn, J. I. Zink, *J. Phys. Chem.* **1989**, *93*, 2129.

[31] J. C. Pouxviel, B. Dunn, J. I. Zink, *J. Phys. Chem.* **1989**, *93*, 2134.

[32] U. Narang, R. Wang, P. N. Prasad, F. V. Bright, *J. Phys. Chem.* **1994**, *98*, 17.

[33] U. Narang, J. D. Jordan, F. V. Bright, P. N. Prasad, *J. Phys. Chem.* **1994**, *98*, 8101.

[34] M. Kryszewski, D. Lapienis, B. Nadolski, *J. Polym. Sci.* **1973**, *11*, 2423.

[35] A. Schonberg, A. Mustafa, W. Asker, *J. Am. Chem. Soc.* **1951**, *73*, 2876.

[36] C. Balny, P. Douzou, C. R. *Acad. Sci. Paris* **1967**, *264*, C-477.

[37] T. R. Evans, A. F. Toth, P. A. Leermakers, *J. Am. Chem. Soc.* **1967**, *89*, 5060.

[38] E. Inoure, T. Nakayama, H. Kodako, *Kogyo Kagaku Zasshi* **1969**, *72*, 2352.

[39] P. de Mayo, A. Safarzadeh-Amiri, S. K. Wong, *Can. J. Chem.* **1984**, *62*, 1001.

[40] R. K. Iler, in *Science of Ceramic Chemical Processing* (L. L. Hench, D. R. Ulrich, eds.), Wiley, New York, 1986, pp. 3.

[41] R. Y. Sheinfain, O. P. Stas, I. E. Neimark, *Kolloidn. Zh.* **1965**, *27*, 916.

[42] B. S. Girgis, *Z. Phys. Chem.* **1973**, *83*, 75.

[43] C. J. Brinker, G. W. Scherer, in: *Sol-Gel Science: The Physics and Chemistry of Sol-Gel Processing*, Academic Press, San Diego, 1990, p. 387.

[44] O. Lev, M. Tsionsky, L. Rabinovich, V. Gletzer, S. Sampath, I. pankratov, J. Gun, *Anal. Chem.* **1995**. *67*, 22A.

[45] O. Lev, *Analusis* **1992**, *20*, 543.

[46] B. C. Dave, B. Dunn, J. S. Valentine, J. I. Zink, *Anal. Chem.* **1994**, *66*, 1120A.

[47] J. E. Lee, S. S. Saavedra, *Anal. Chim. Acta* **1994**, *285*, 265.

[48] J. M. Barrero, C. Cámara, M. C. Pérez-Conde, C. San José, L. Fernández, *Analyst* **1995**. *120*, 431.

[49] U. Narang, R. A. Dunbar, F. V. Bright, P. S. Prasad, *Appl. Spectrosc.* **1993**, *47*, 1700.

[50] C. A. Browne, D. H. Tarrant, M. S. Olteanu, J. W. Mullens, E. L. Chronister, *Anal. Chem.* **1996**, *68*, 2289.

[51] G. O'Keeffe, B. D. MacCraith, A. K. McEvoy, C. M. Mc-Donagh, J. F. McGilp, *Sens. Actuators B* **1995**, *29*, 226.

[52] B. D. MacCraith, C. M. McDonagh, G. O'Keeffe, E. T. Keyes, J. G. Vos, B. O'Kelly, J. F. Mc Gilp, *Analyst* **1993**, *118*, 385.

[53] R. A. Dunbar, J. J. Jordan, F. R. Bright, *Anal. Chem.* **1996**, 68, 604.

[54] D. Anvir, S. Braun, M. Ottolenghi, in: *Supramolecular Architecture: Synthetic Control in Thin Films and Solids* (T. Bein, ed.), *American Chemical Society Symposium Series 499,* ACS, Washington, D. C. 1992.

[55] S. A. Yamanaka, F. Nishida, L. M. Ellerby, C. R. Nishida, B. Dunn, J. S. Valentine, J. I. Zink, *Chem. Mater.* **1992**, *4*, 495.

[56] S. A. Yamanaka, B. Dunn, J. S. Valentine, J. I. Zink, *J. Am. Chem. Soc.* **1995**, *117*, 9095.

[57] D. J. Blyth, J. W. Aylott, D. J. Richardson, D. A. Russell, *Analyst* **1995**, *120*, 2725.

[58] K. E. Chung, E. H. Lan, M. S. Davidson, B. S. Dunn, J. S. Valentine, J. I. Zink, *Anal. Chem.* **1995**, *67*, 1505.

[59] Z. Suprynowicz, B. Buszewski, R. Ludkowski, A. L. Dawidowicz, *J. Chromatogr.* **1988**, *446*, 347.

[60] S. M. Fields, *Anal. Chem.* **1996**, *68*, 2709.

[61] B. Dunn, G. C. Farrington, B. Katz, *Solid State Ionics* **1994**, *70/71*, 3.

[62] J. M. Bell, G. B. Smith, D. C. Green, J. Barczynska, L. Evans, K. A. MacDonald, G. Voelkel, B. O. West, L. Spiccia, *SPIE* **1993**, *2017*, 132.

[63] J. Göttsche, A. Hinsch, V. Wittwer, *Sol. Energy Mater. Sol. Cells* **1993**, *31*, 415.

[64] M. A. Macêdo, M. A. Aegerter, *J. Sol-Gel Sci. Technol.* **1994**, *2*, 667.

[65] J. Lemerle, L. Nejem, *J. Inorg. Nucl. Chem.* **1980**, *42*, 17.

[66] R. Baddour, J. P. Pereira-Ramos, R. Messina, J. Perichon, *J. Electroanal. Chem.* **1990**, *277*, 359.

[67] F. Chaput, B. Dunn, P. Fuqua, K. Salloux, *J. Non-Cryst. Solids* **1995**, *188*, 11.

[68] K. Salloux, F. Chaput, H. P. Wong, B. Dunn, M. W. Breiter, *J. Electrochem. Soc.* **1995**, *142*, L191.

[69] R. Baddour-Hadjean, J. Farcy, J. P. Periera-Ramos, *J. Electrochem. Soc.* **1996**, *143*, 2083.

[70] U. L. Ŝtangar, B. Orel, I. Gtrabec, B. Ogorevc, K. Kalcher, *Sol. Energy Mater. Sol. Cells* **1993**, *31*, 171.

[71] M. Guglielmi, P. Colombo, G. Battaglin, A. Boscolo-Boscoletto, *Eur. Mater. Res. Soc. Monogr.* **1992**, *5*, 111.

[72] B. J. Hwang, D. T. Shieh, A. S. T. Chiang, *J. Chin. Inst. Chem. Eng.* **1994**, *25*, 127.

[73] M. El Baydi, G. Poillerat, J.-L. Rehspringer, J. L. Gautier, J.-F. Koenig, P. Chartier, *J. Solid State Chem.* **1994**, *109*, 281.

[74] P. Audebert, c. Demaille, C. Sanchez, *Chem. Mater.* **1993**, *5*, 911.

[75] Y. Tatsu, K. Yamashita, M. Yamaguchi, S. Yamamura, H. Yamamoto, S. Yoshikawa, *Chem. Lett.* **1992**, 1615.

[76] V. Glezer, O. Lev, *J. Am. Chem. Soc.* **1993**, *115*, 2533.

[77] I. Pankratov, O. Lev, *J. Electroanal. Chem.* **1995**, *393*, 35.

[78] S. Sampath, O. Lev, *Anal. Chem.* **1996**, *68*, 2015.

[79] J. Wang, P. V. A. Pamidi, D. S. Park, *Anal. Chem.* **1996**, *68*, 2705.

[80] B. C. Dave, B. Dunn, J. S. Valentine, J. I. Zink, in: *Access in Nanoporous Materials* (T. J. Pinnavaia and M. F. Thorpe, eds.), Plenum Press, New York, 1995, pp. 141–159.

[81] P. J. Kulesza, *J. Electroanal. Chem.* **1990**, *298*, 103.

[82] R. K. Jaworski, J. A. Cox, *Electrochim. Acta* **1992**, *37*, 5.

[83] J. I. Dulebohn, S. C. Haefner, K. A. Bergland, K. R. Dunbar, *Chem. Mater.* **1992**, *4*, 506.

[84] D.-D. Lee, S.-D. Choi, K.-W. Lee, *Sens. Actuators B* **1995**, *24/25*, 607.
[85] K. Kimura, T. Sunagawa, M. Yokoyama, *Chem. Comm.* **1996**, 745.
[86] C. C. Hsueh, M. M. Collinson, *J. Electroanal. Chem.* in press, **1997**.
[87] A. Yasuda, N. Yamaga, K. Doi, T. Fujioka, S. Kusanagi, *J. Electrochem. Soc.* **1992**, *139*,1091.
[88] S. B. Lee, A. Cocco, D. Keyvani, G. J. Maclay, *J. Electrochem. Soc.* **1995**, *142*, 157.
[89] B. N. Oliver, L. A. Coury, J. O. Egekeze, C. S. Sosnoff, Y. Zhang, R. W. Murray, C. Keller, M. X. Umana, in: *Biosensor Technology: Fundamentals and Applications* (R. P. Buck, W. E. Hatfield, M. X. Umana, E. F. Bowden, eds.), Marcel Dekker, New York 1990, pp. 117–135.
[90] J. A. Cox, K. S. Alber, M. E. Tess, T. E. Cummings, W. Gorski, *J. Electroanal. Chem.* **1995**, *396*, 485.
[91] J. A. Cox, K. S. Alber, *J. Electrochem. Soc.* **1996**, *143*, L126.
[92] K. S. Alber, *Ph.D. Dissertation*, Miami University, Oxford, OH, 1996.

Received October 19, 1996.